WATER RESOURCES RESEARCH, VOL. 33, NO. 4, PAGES 853–864, APRIL 1997

Stochastic modeling of transect-to-transect properties of Great Basin rangeland streams

Thomas J. Myers and Sherman Swanson
Department of Environmental and Resource Sciences, University of Nevada, Reno

Abstract. We developed a transect-to-transect stochastic model of stream width and pools. The model included Markov chains for transect-to-transect transitions among pools, nonpools, and part pools, a two-parameter beta distribution for pool fraction when the transect is a partial pool, and a two-parameter gamma distribution to model standardized widths. The model accurately reproduced the mean and standard deviation of both width and transect-based measures of pool area. However, the model smoothed the distributions thereby reducing the skewness of the observed data. The physical tendency for streams to have very few transects that are almost, but not totally, all pool or nonpool implies that stochastic models based on continuous distributions will have more density in the tails than observed on the stream. The model represented odd-shaped empiric distributions of pool area which indicates it is very flexible and can accurately model a variety of streams.

Introduction

The variance of width or pool area (PA) measurements depends on the inherent variability of width and the pool-riffle sequence along the measured stream reach and measurement precision [*Myers*, 1996]. Measurement precision is partly a function of a surveyor's ability to read a tape measure, recognize water or channel width [*Williams*, 1978], and determine the boundaries of a pool [*Robison and Kaufman*, 1994; *Hankin and Reeves*, 1988] and inherent equipment errors. Measurement precision increases with training, experience, and care. However, physical longitudinal differences due to coarse woody debris [*Keller and Swanson*, 1979; *Robison and Beschta*, 1990], dominant vegetation [*Murgatroyd and Ternan*, 1983], soil type [*Phillips and Harlin*, 1984], and the location within the pool-riffle sequence [*Harvey*, 1975; *Richards*, 1976] lead to inherent variability.

Sampling precision of width and PA, expressed as the coefficient of variation (CV), is a function of the number and spacing of transects [*Myers*, 1996]. A transect is a cross section perpendicular to the channel centerline. Stochastic homogeneity of a stream reach is the condition that all measured parameters be drawn from the same population such that moments do not depend on the location along the reach. Sampling from two or more adjacent inhomogeneous reaches increases the variance of any estimates. Stochastic homogeneity is a function of scale whereby clusters of pools or short lengths of narrow or wide streams may be small parts of longer reaches. Estimates of variability by *Myers* [1996] are probably low because homogeneous reaches are short and do not represent the full range possible for streams of a given range of stochastic parameters.

The first purpose of this paper is to model the width and PA of streams using transect-to-transect and at-a-transect stochastic properties of streams. Specifically, we modeled the change of pool category (no pool, pool, or part pool) from transect to transect with Markov chains, at-a-transect properties of pool fraction with a two-parameter beta distribution, and width in a conditional two-parameter gamma distribution model. This allows simulation of perfectly homogeneous stream reaches based on transect-to-transect processes completely specified by stochastic model parameters. Using this model, it is possible to explore the full range of expected measurement precision for various sampling schemes.

The second purpose is to determine whether relations exist between distribution parameters and basic stream morphology. If so, managers could use this model to vary their survey techniques based on stream morphology.

Paper number 96WR04015.
0043-1397/97/96WR-04015$09.00

Background

Stochastic modeling and simulation has much precedence in geomorphology [*Leopold and Langbein*, 1962; *Price*, 1974; *Shreve*, 1974; *Kirchner*, 1993]. However, the modeling of channel width has generally been limited to deterministic power function relationships of width and basin area [*Klein*, 1981] or flow rate [*Pickup and Reiger*, 1979] ignoring randomness. Exceptions include *Rendell and Alexander* [1979] who found that small-scale variability in ephemeral channel width and depth due to channel forming processes, occurring during unsteady flow, confounded assessments of deterministic relations. Using the same data, *Alexander and Rendell* [1995] introduced randomness into the modeling of width with models to separate white noise from deterministic trends.

Markov chains have been used in hydrology primarily to simulate climate [*Gabriel and Neumann*, 1962; *Haan et al.*, 1976], drought [*Thompson*, 1990], or flood stages [*Yakowitz*, 1985; *Yapo et al.*, 1993]. In stream morphology, *Myers and Swanson* [1996] used transition probabilities to detect tendencies in stream type changes due to flooding or trends in sequences of habitat units [*Grant et al.*, 1990].

Because the two-parameter beta distribution ranges from 0 to 1, it is ideal for modeling fractions and proportions [*Law and Kelton*, 1991] that are not uniformly distributed. Although *Mielke and Johnson* [1974] suggested the beta distribution had the same capability as the lognormal or gamma distribution for modeling precipitation and streamflow, it has found limited use in hydrology. Exceptions include a model of the fraction of

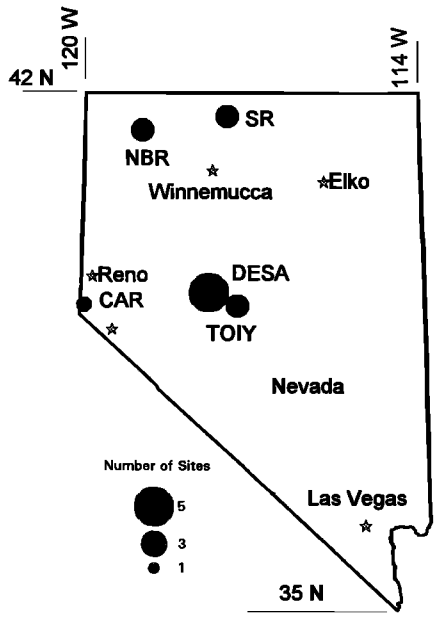

Figure 1. Location map. The size of circles represents the number of sites in each mountain range. SR, Santa Rosa Mountains; NBR, North Black Rock Mountains; DESA, Desatoya Mountains; TOIY, Toiyabe Mountains; CAR, the Carson Range. See Table 1 for which site is located in each mountain range.

daily precipitation that fell as rain or snow [*Yevjevich and Harmancioğlu*, 1990] and use of the distribution function as the shape of cumulative hyetographs [*Acreman*, 1990]. Similar to these uses, we used the beta distribution to model fractions from 0 to 1.

Study Area

We used 12 long (>67 widths, 83% > 125 widths) stream segments in five mountain ranges of central and northwestern Nevada (Figure 1). All are within the basin and range geologic province [*Stewart and Carlson*, 1978]. Dominant vegetation types range from sagebrush steppe to pinyon-juniper woodlands. Riparian vegetation includes species from grasses and sedges to shrubs and trees.

Our study sites represent three general stream types [*Rosgen*, 1994] prevalent in Nevada [*Myers and Swanson*, 1991]. We classified sites according to general *Rosgen* [1994] types only. Thus classification was based on cross-sectional properties (channel width/depth and entrenchment) and sinuosity only. B-type streams are moderately entrenched and sinuous and have a moderate width/depth ratio (>12). C-type streams are slightly entrenched, have a high width/depth ratio, and are very sinuous. E-type streams are similar to C-type streams except they have a narrow channel (low width/depth ratio). All streams have a predominately gravel substrate (2–64 mm). Table 1 describes each study reach. *Rosgen* [1994] indicates predominate gradients for general type (2–4% for B and <2% for C and E types, respectively), but gradients in Table 1 for some B- and C-types exceed the expected values.

Methods

We measured cross-sectional properties at transects perpendicular to the active channel spaced between 1 and 1.5 channel widths. Reach lengths varied from 63 to 251 transects (Table 1) and were intended to be stochastically homogeneous.

During base flow at each transect we measured channel and water width, maximum channel depth and width at twice the maximum channel depth (to determine stream type), and the width of pools within the transect. The fraction of water width that is a pool, defined as the width of pool divided by the water width, is the pool fraction (PF). Base flow exists when streamflow consists almost entirely of groundwater return flow [*Mosley and McKerchar*, 1993]. We assumed that base flow was occurring when spring runoff had ceased and flow rates had become essentially constant. In Nevada, base flow occurs for up to 300 days of the year [*Myers and Swanson*, 1996]. The top of active channel is the point where an area-width curve substantially changes slope [*Williams*, 1978] as estimated in the field at each transect. Vegetation, scour marks, bar height, and

Table 1. Characteristics of Study Sites

Number	Stream	n	Channel Width, m Mean	(s.d.)	Water Width, m Mean	(s.d.)	Transect Spacing, m	(widths)	$\rho(cw)_1$	$\rho(ww)_1$	Gradient	PA	Moutain Range	General *Rosgen* [1994] Stream Type
1	Smith U	199	1.96	(0.74)	1.24	(0.39)	2.0	1.02	0.704[a]	0.273[a]	0.150	0.26	DESA	B
2	Smith D	163	2.09	(0.58)	1.23	(0.30)	3.0	1.43	0.471[a]	0.061	0.007	0.47	DESA	C
3	Reese R	63	4.92	(0.94)	3.04	(0.55)	8.0	1.63	0.427[a]	0.147	0.003	0.50	TOIY	C
4	Big Den D	151	1.38	(0.53)	0.69	(0.24)	2.0	1.45	0.417[a]	0.128	0.060	0.18	DESA	C
5	Big Den U	150	1.53	(0.54)	1.08	(0.42)	2.0	1.31	0.475[a]	0.365[a]	0.125	0.30	DESA	B
6	Big Mead.	251	1.15	(0.45)	0.81	(0.32)	2.0	1.74	0.415[a]	0.241[a]	0.008	0.20	CAR	E
7	Cabin D	104	2.34	(0.99)	1.40	(0.52)	2.0	0.85	m	0.567[a]	0.008	0.76	SR	C
8	Cabin U	192	1.34	(0.46)	0.86	(0.26)	2.0	1.49	0.566[a]	0.134	0.031	0.45	SR	B
9	Mahogany	169	2.62	(0.73)	1.60	(0.53)	3.0	1.14	0.432[a]	0.206[a]	0.019	0.40	NBR	C
10	Summer Cp	126	1.94	(0.47)	1.44	(0.42)	3.0	1.55	0.060	0.035	0.054	0.23	NBR	B
11	Washington	148	2.41	(0.57)	1.97	(0.54)	3.0	1.24	0.402[a]	0.367[a]	0.060	0.36	TOIY	B
12	Willow	199	1.63	(0.58)	1.14	(0.38)	2.0	1.23	0.495[a]	0.094	0.076	0.33	DESA	B

Standardized spacing is transect spacing divided by mean channel width. s.d., standard deviation; $\rho(\ )_1$, lag 1 autocorrelation for channel width (CW) or water width (WW). PA, pool area (equation (1)) where n equals the total number of transects. m, missing; Gradient, hydraulic gradient; SR, Santa Rosa Mountains; NBR, North Black Rock Mountains; DESA, Desatoya Mountains; TOIY, Toiyabe Mountains; CAR, the Carson Range. See Figure 1 for location.

[a] $P \leq 0.1$.

topographic break points aided delineation [*Leopold*, 1994]. All width measurements were standardized by the average water width so that units in the model are widths. This allows comparison among streams of different size. Along the plan of the reach we measured sinuosity of the center of the active channel and hydraulic gradient.

Pool area is the fraction of stream surface classified as a pool using methods of *Grant et al.* [1990]. When measured with transects, PA may be defined as

$$PA = \frac{\sum_{i=1}^{n} PF_i(WW_i)}{\sum_{i=1}^{n} WW_i} = \frac{\sum_{i=1}^{n} PF_i(WW_i)}{n(\overline{WW})} \quad (1)$$

where n is the number transects per study site and WW_i is water width for transect i. (Table 1 contains n and PA). A pool is a distinct habitat unit with hydraulic gradient less than the stream average and subcritical flow conditions except for an entry jet which may cause supercritical flow up to 15% of the surface. On the basis of this definition of PA any transect-based stochastic model must include WW and PF. Water width, measured at base flow conditions, represents the low-flow channel which may be a stable indicator of basin conditions [*Richards*, 1982].

Model Development

Stream morphology variables of interest at evenly spaced transects are WW and PF. We theorized that changes in WW and PF from transect to transect are a Markov process where conditions at a transect depend only on conditions at the transect immediately upstream. This assumption is based on the insignificant autocorrelation of width for two or more lags [*Richards*, 1976; *Myers*, 1996] and the variability of width through pool-riffle sequences forced by coarse woody debris (CWD) [*Robison and Beschta*, 1990]. Transitions between pools, nonpools, and part pools are a three-state Markov chain. In the range $0 < PF < 1$, histograms of PF suggest a density function with variable skewness and means substantially varying from 0.5. Thus PF does not follow a uniform distribution. Therefore we theorized that PF would follow a two-parameter beta distribution similar to the distribution of precipitation as a fraction of rain when there was a mixture of precipitation types [*Yevjevich and Harmancioğlu*, 1990]. Overall, then, PF follows a combined bernouli/beta distribution. As reported below, we tested for and found no significant conditional distributions of PF dependent on WW for $0 < PF < 1$. We modeled width as a gamma distribution conditioned on the transect category (pool, nonpool, or part pool).

Markov Chain Model

A first-order Markov chain is a stochastic process (X_n, $n = 0, 1, 2, \ldots$) that takes on a countable number of possible values with states (0, 1, 2, ...) [*Ross*, 1982]. It has the property

$$P(X_{n+1} = j | X_n = i_n, X_{n-1} = i_{n-1}, \cdots, X_1 = i_1, X_0 = i_0) = P_{ij} \quad (2)$$

for all states $i_0, i_1, \cdots, i_{n-1}, i_n, j$, and $n \geq 0$. For modeling PF there are three states 0, 1, or 2 representing nonpool, pool, or part pool, respectively.

Table 2. Transition Probability Matrix and Total Probability That a Transect is in a Given State Irrespective of the Previous State

Reach	State	State 0	State 1	State 2	Total Probability
Smith U	0	0.569	0.157	0.274	0.510
	1	0.281	0.312	0.406	0.328
	2	0.531	0.094	0.375	0.162
Smith D	0	0.403	0.492	0.104	0.398
	1	0.414	0.414	0.171	0.428
	2	0.345	0.345	0.310	0.175
Reese R	0	0.357	0.357	0.286	0.210
	1	0.200	0.560	0.240	0.419
	2	0.130	0.304	0.565	0.371
Big Den D	0	0.612	0.047	0.341	0.567
	1	0.375	0.000	0.625	0.053
	2	0.526	0.070	0.404	0.380
Big Den U	0	0.527	0.135	0.338	0.500
	1	0.464	0.250	0.286	0.187
	2	0.479	0.229	0.292	0.313
Big Meadow	0	0.344	0.422	0.234	0.256
	1	0.194	0.674	0.132	0.576
	2	0.333	0.476	0.191	0.168
Cabin D	0	0.118	0.706	0.177	0.155
	1	0.167	0.621	0.212	0.641
	2	0.150	0.650	0.200	0.204
Cabin U	0	0.467	0.359	0.174	0.472
	1	0.452	0.425	0.123	0.378
	2	0.536	0.321	0.143	0.150
Mahogany	0	0.441	0.265	0.294	0.411
	1	0.308	0.423	0.269	0.310
	2	0.479	0.250	0.271	0.280
Summer Camp	0	0.621	0.091	0.288	0.536
	1	0.529	0.294	0.177	0.136
	2	0.405	0.143	0.452	0.328
Washington	0	0.320	0.340	0.340	0.347
	1	0.389	0.278	0.333	0.245
	2	0.344	0.148	0.508	0.408
Willow	0	0.543	0.219	0.238	0.525
	1	0.510	0.347	0.143	0.252
	2	0.500	0.227	0.273	0.222

State 0, 1, and 2 are no, complete, and part pool. Table 1 contains the total number of transects.

Conceptually, additional states could be added by subdividing the interval $0 < PF < 1$ similar to *Haan et al.* [1976] for daily rainfall or *Yapo et al.* [1993] for flow categories below flood levels. We did not do this for two reasons. First, as will be discussed below, the beta (α_1, α_2) distribution described this range very well. Second, the number of data points needed to adequately determine transition probabilities increases exponentially [*Yapo et al.*, 1993] with additional states.

The transition probability matrix (TPM) is a 3×3 matrix with

$$P_{ij} = P(X_{t+1} = j | X_t = i) \qquad \text{for } i, j = 0, 1, 2 \quad (3)$$

and

$$\sum_{i=0}^{2} P_{ij} = 1 \qquad \text{for each } j \quad (4)$$

Elements of the TPM are estimated as n_{ij}/n_i, where n_{ij} is the number of transitions from state i (rows of the matrix) to state j (columns) and n_i is the number of observations in state i. In a TPM, i and j represent rows and columns, respectively. Table 2 contains the TPM and total probability P_t for 12 reaches used in the modeling.

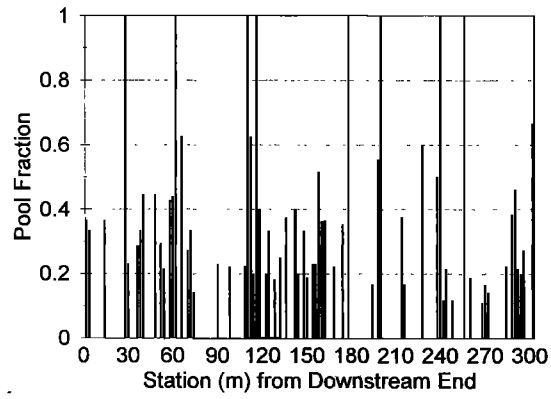

Figure 2. Location of pools as represented by pool fraction at a transect on Big Den D.

Total probability reflects pool area. For example, Cabin D and Big Den D have the highest and lowest PA (Table 1) and P_1 (Table 2), respectively. Two of the higher P_2 values, representing part pools, occurred on type C4 reaches Reese R and Big Den D. These streams have free-form pool-riffle sequences with very little debris and few boulders. However, corner pools have submerged bars on the inner curves classified as riffles. The highest P_2 occurred on Washington C which has many boulders leading to partial pools. There are no apparent differences in part pools between B and C types or trends with stream size. The primary similarity among streams with few part pools is a lack of bars (deposition) and boulders (for pocket pools).

Reaches with high P_0 tended to be type B4. Of five reaches with $P_0 \geq 0.5$, only Big Den D is not B4 (four of six B4 reaches have $P_0 \geq 0.5$). This suggests that nonpools dominate B4 streams. The high partial pools on some B4 reaches, which increased their PA substantially, suggest that random features such as boulders or coarse woody debris (CWD) are necessary for pool formation [*Myers and Swanson*, 1994] on these stream types.

Tendencies for transects with pools to follow one another (P_{11} substantially exceeding P_1) suggest pool area clustering. This is either a clustering of pools, a prevalence of short nonpool reaches not often sampled by transects at our spacings, or a tendency toward long pools. Eight reaches showed this tendency (Table 2), but there were no obvious tendencies among specific stream types. However, Big Den U, Cabin U, Mahogany, Summer Camp, Washington, and Willow were predominately tree- and shrub-lined. All but Mahogany had substantial numbers of boulders. This suggests that structural features such as boulders and CWD may not be random and may cause clusters of pools at short spacings. Reese R and Big Meadow are opposite having very long, regularly spaced pools such that several transects intersect each pool and transects in nonpools are followed by pools. The tendency for nonpool transects to repeat on six reaches (Table 2) corroborates these observations. Big Den D exhibited an opposite tendency ($P_{11} \ll P_1$) toward short, irregularly spaced pools (Figure 2).

We did not use higher step transition matrices because the transition probabilities approached the total probability at the second step. That is,

$$P_{ij}^2 = P(X_{n+m} = j | X_m = i) \rightarrow P_i \tag{5}$$

This suggested there was no correlation or cyclicity for pools at lags higher than one analogous to the lack of higher-order correlation of width [*Myers*, 1996].

Distribution of the Pool Fraction

If transects were all either pools or nonpools, there would have been only two states in the Markov chain and PF, equaling 0 or 1, would draw from a Bernouli distribution. However, 29% of transects over all reaches are not complete pools or nonpools. The three states chosen here imply a conditional combined discrete and continuous distribution:

$$f(\mathrm{PF}) = p_0 \qquad \mathrm{PF} = 0 \tag{6}$$

$$f(\mathrm{PF}) = p_2 f(\mathrm{PF} | 0 < \mathrm{PF} < 1) \qquad 0 < \mathrm{PF} < 1 \tag{7}$$

$$f(\mathrm{PF}) = p_1 \qquad \mathrm{PF} = 1 \tag{8}$$

where p_0 and p_1 are the probabilities that PF equals 0 or 1, respectively, p_2 is the probability that $0 < \mathrm{PF} < 1$. Because $f(\mathrm{PF}) \rightarrow 0$ as $\mathrm{PF} \rightarrow 0$ or 1 in the range $0 < \mathrm{PF} < 1$ and because of its flexibility in describing shapes between 0 and 1 [*Law and Kelton*, 1991], beta (α_1, α_2) is a logical choice to describe PF.

$$f(\mathrm{PF} | 0 < \mathrm{PF} < 1) = \frac{\mathrm{PF}^{\alpha_1 - 1}(1 - \mathrm{PF})^{\alpha_2 - 1}}{\beta(\alpha_1, \alpha_2)} \tag{9}$$

The beta function $\beta(\alpha_1, \alpha_2)$ is

$$\beta(\alpha_1, \alpha_2) = \frac{\Gamma(\alpha_1)\Gamma(\alpha_2)}{\Gamma(\alpha_1 + \alpha_2)} \tag{10}$$

and $\Gamma(x)$ is the gamma function. Parameter estimation is by the method of moments (MME).

$$\alpha_1 = \overline{\mathrm{PF}}\left(\frac{\overline{\mathrm{PF}}(1 - \overline{\mathrm{PF}})}{S_{\mathrm{PF}}^2} - 1\right) \tag{11}$$

$$\alpha_2 = (1 - \overline{\mathrm{PF}})\left(\frac{\overline{\mathrm{PF}}(1 - \overline{\mathrm{PF}})}{S_{\mathrm{PF}}^2} - 1\right) \tag{12}$$

where $\overline{\mathrm{PF}}$ and S_{PF} are the sample mean and standard deviation for the fraction $0 < \mathrm{PF} < 1$.

We tested the suitability of the beta distribution with a χ^2 goodness-of-fit test for H_0: data for individual reaches are independent identically distributed (IID) random variables with distribution function beta (α_1, α_2). Rejecting H_0 when $\chi^2 > \chi^2_{k-1,1-\alpha}$ and k is the number of categories chosen to be equiprobable with expected value np ranging from 6 to 8 and with a minimum k equal to 4 [*Law and Kelton*, 1991], we accepted the chosen distribution on 11 of 12 study reaches (Table 3). Spearman rank correlations of PF and WW in the range $0 < \mathrm{PF} < 1$ were small and variously positive or negative indicating no conditional relationship.

For example, Smith D shows an excellent fit throughout the range (Figure 3a). Mahogany still fits a beta distribution (Figure 3b) while differing at $\mathrm{PF} > 0.4$ because the primary difference was limited to one category. However, Smith U had few observations as PF approaches 0 which led to rejection of the beta distribution (Figure 3c). The lowest category for Smith U, (0, 0.1), was lower than any category for any of the reaches. Most reaches tended to fewer than expected transects in very low categories because very small pools rarely exist on these streams. There is probably a minimum pool width. A PF = 0.1 in our stream size range suggests a minimum width for pools near 0.2 m.

Table 3. Beta Distribution Parameters (α_1, α_2) for PF and χ^2 Goodness-of-Fit Comparison With Empirical Distributions in the Interval $0 < PF < 1$

Reach	n	k	α_1	α_2	χ^2	P	μ_{mo}	$r_{pf,w}$
Smith U	65	10	1.77	3.72	19.2	0.024	0.221	0.094
Smith D	29	4	3.50	6.36	0.10	0.992	0.318	0.208
Reese R	23	4	2.79	10.3	4.65	0.199	0.161	0.097
Big Den D	58	8	3.14	6.95	8.76	0.270	0.264	−0.103
Big Den U	48	6	3.61	4.62	3.25	0.662	0.419	−0.303
Big Meadow	42	6	2.14	2.53	1.43	0.921	0.427	−0.090
Cabin D	21	4	2.43	2.22	0.14	0.987	0.540	0.278
Cabin U	29	4	2.25	4.01	2.03	0.566	0.293	0.108
Mahogany	48	6	1.55	2.32	5.50	0.358	0.294	−0.053
Summer Camp	42	6	1.95	4.05	6.57	0.255	0.238	−0.221
Washington	61	8	1.94	3.88	2.87	0.897	0.246	0.005
Willow	44	6	2.20	3.58	2.91	0.714	0.318	0.155

PF, pool fraction; n, number of transects; k, number of categories in the goodness-of-fit test; P, significance probability; μ_{mo}, mode calculated from the hypothesized population distribution; $r_{pf,w}$, Spearman rank correlation.

The mode of the beta distribution [*Law and Kelton*, 1991]

$$\mu_{mo} = \frac{\alpha_1 - 1}{\alpha_1 + \alpha_2 - 2} \tag{13}$$

indicates that if $\alpha_1 < \alpha_2$, the mode is less than 0.5. The modes for our study reaches clustered between 0.22 and 0.43 with one exception exceeding 0.5 and another being less than 0.2 (Table 3). The mode approaches 0 or 1 as one parameter becomes substantially larger than the other. The density becomes more leptokurtic (peaked) as the parameters become larger. Parameters for reaches Smith D, Big Den D, and Big Den U tended to be larger than the others and indicated a tendency toward concentration (peaked density) near the mode. Reese R had a very large α_2 indicating a peaked concentration of values at low PF. This is the widest reach and had a distinct free-formed pool-riffle sequence. The tendency for low PF values (in the $0 < PF < 1$ range) suggests that pool units have narrow extensions into adjoining riffles. In general, we found great flexibility in the shape of the density function for the chosen range of data as did *Haktanir and Sezen* [1990] for unit hydrographs.

Distribution of Water Width

Tested with one-way analysis of variance (ANOVA), water width differed among pool categories ($p < 0.05$) on all reaches but Reese R. Water width was highest on part pools on all reaches except Smith D where width without pools was slightly, but not significantly, higher (Figure 4). Transects with overlapping habitat types ($0 < PF < 1$) were wider because velocities across the transect vary more than pools or nonpools. Complete pools were narrower and deeper than other categories. Part pools were deeper than, but closer to, nonpools than to pools. Most partial pools occurred at the downstream shallow end of pools where they transitioned into riffles or rapids. The lower velocity in the pool portion of part pool transects requires a higher conveyance capacity frequently leading to a wider stream. Flow below pools diverges becoming wider followed by convergence in a riffle or rapid prior to further narrowing, and scouring, into a pool. The deepest part corresponds to the point of maximum convergence where scour usually creates a uniformly deep section [*Keller*, 1971].

The two-parameter gamma distribution can have a mode close to 1, is bounded on the left by 0, and ranges to infinity on the right. It models the right skewness caused by left bounding. We modeled standardized water width (ww); therefore the $\overline{ww}$ was near 1.0, and ww ranged from less than 0.5 to about 2.5. We conditioned the model on the three pool categories. The gamma distribution is

$$f(WW) = \frac{\beta^{-\alpha} WW^{\alpha-1} e^{-ww/\beta}}{\Gamma(\alpha)} \qquad WW > 0$$
$$f(WW) = 0 \qquad \text{otherwise} \tag{14}$$

where α and β are parameters estimated by MME.

We tested the fit with a χ^2 goodness-of-fit test for H_0: the data for individual reaches are IID random variables with distribution function gamma (α, β). We rejected H_0 when $\chi^2 > \chi^2_{k-1,1-\alpha}$ ($\alpha = 0.10$) using $k = 10$ categories chosen to be equiprobable [*Law and Kelton*, 1991]. We accepted the chosen distribution on 11 of 12 study reaches for complete and partial pools and on 10 of 12 reaches for no pools (Table 4). The worst fit occurred on Cabin U for no pools because of a very irregular distribution with observations clustering at several values as seen by the steepening of the observed distribution (Figure 5). This clustering would not cause rejection of H_0 if fewer categories were used.

Simulation Model

Parameters needed for the model were α_1 and α_2 in the beta distribution for PF when $0 < PF < 1$, three α values and β values in the gamma distributions for width for three pool categories. The number of states, PF categories, and order of the Markov chain are also parameters but predetermined by the model structure.

The pool category for the first simulated transect is determined by comparing a random number chosen from $U(0, 1)$ with the total probabilities. $U(0, 1)$ is the uniform distribution from 0 to 1 not inclusively. If the category is a partial pool, PF is chosen from the beta distribution using a new random number; otherwise, PF equals 0 or 1. Then, the width is chosen from the gamma distribution for the appropriate pool category. The pool category of the following transect depends on the pool category of the current transect and is selected with another random number and the TPM. *Myers* [1996] provides a simulation flow diagram. The simulation requires an initial

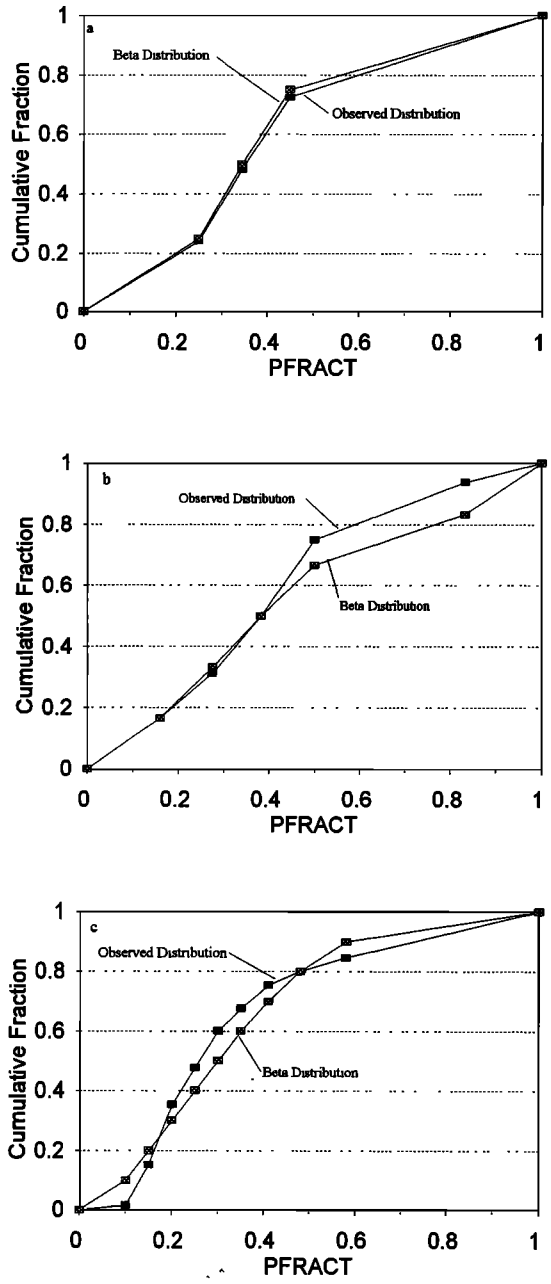

Figure 3. Beta distribution and observed distribution of pool fraction (PFRACT) for select streams, 0 < PFRACT < 1. (a) Smith D, (b) Mahogany, and (c) Smith U.

seed (a very large integer) which is updated internally by the program each time a random number is chosen. Each generated value is based on a new random number. Fortran V subroutines for random number generation from *Press et al.* [1992] were used. The result of the model is a stochastically homogeneous, digital stream of a length chosen by the user represented by transects similar to field measurements.

Verification

Stochastic models do not model deterministic processes. Rather, they model the variability of basic form measurements of the process, in this case, width and PF and by extension, PA. We simulated reaches 8000 transects long using parameters for each of the 12 sites. The input distributions and TPM should be, and were, reproduced exactly within roundoff error. This does not verify that the streams are similar to those measured, only that we coded the distributions and TPMs properly.

An accurate stochastic model would reproduce the overall mean, variance, and skew of width and PA for various sampling strategies. Modeled widths for all reaches were near perfect. The standard deviations were in close agreement, but skew values were underestimated by up to 50% (Figure 6). Simulation of many transect widths had a smoother distribution than the observed values (e.g., Figure 7) and lower skewness coefficients. For example, there is little difference between the fractions for observed width categories [0.6, 0.7) and [0.7, 0.8), but fractions from the simulation differed by 80% (Figure 7). Agreement improves near the mean of 1.0. As found for precipitation and streamflow [*Mielke and Johnson*, 1974; *Bobée and Ashkar*, 1991], the gamma distribution is not perfect in the tails because of limited observations.

The simulation model allows calculation of PA based on any sampling scheme using systematic transects. We chose two schemes that would yield high CV for better comparison to represent various properties of the transect series. Both the observed and simulated streams were subsampled starting at the upstream transect and progressing downstream. Separate PA values were calculated according to (15) and (16) starting at each transect.

$$\mathrm{PAGAWS} = \frac{\sum_{t=1}^{5} \mathrm{WW}_{t+4(t-1)}\mathrm{PF}_{t+4(t-1)}}{\sum_{t=1}^{5} \mathrm{WW}_{t+4(t-1)}} \tag{15}$$

This sampling resembles the General Aquatic Wildlife System (GAWS) sampling procedure [*U.S. Forest Service (USFS)*, 1985] by using five transects separated by four transects (with spacing ranging from 1 to 1.5 widths which range from 1 to 5 m, spacing is from 4 to 20 m; GAWS spacing is 15 m without regard to size). The second PA sampling scheme used adjacent transects to preserve persistence in width and pools between adjacent transects:

$$\mathrm{PA5TR} = \frac{\sum_{t=1}^{5} \mathrm{WW}_t\mathrm{PF}_t}{\sum_{t=1}^{5} \mathrm{WW}_t} \tag{16}$$

From the 8000 simulated transects, (15) and (16) resulted in 7984 and 7996 PA representations, respectively. We compared simulated and observed mean, standard deviation and skewness, and overall distributions for each PA over all reaches. Relative accuracy of the simulation of moments was determined using a sum of squared differences coefficient [*Singh*, 1988].

$$\mathrm{SS} = \sum_{i=1}^{12} (Y_{\mathrm{obs}}(i) - Y_{\mathrm{exp}}(i))^2 \tag{17}$$

The mean, standard deviation, or skewness coefficient is represented by Y, and 12 is the number of stream reaches com-

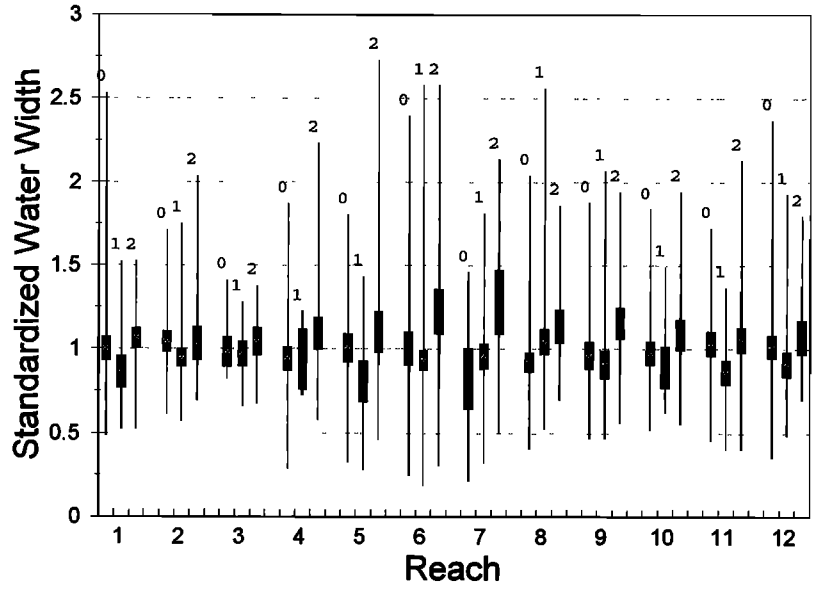

Figure 4. Comparison of standardized water width among stream reaches. 0, 1, and 2 are nonpools, pools, and part pools, respectively.

pared. Observed and simulated distributions of PA were also compared using a Kolmogorov-Smirnoff goodness-of-fit test [*Sokal and Rohlf*, 1981]. This comparison tests the null hypothesis, H_0: observed and simulated PA values are described by the same distribution. H_0 is rejected if the significance probability p is less than 0.10 for n equal to the number of PA observations on the actual reach. The test statistic D is MAX $|P_{PR}(PR) - S_{PR}(PR)|$ or the maximum deviation between distributions [*Haan*, 1977].

Overall, mean and standard deviation were well reproduced, and the skewness coefficient was poorly reproduced by the model (Figures 8 and 9, for PA5TR, SS = 0.0114, 0.0037, and 3.513 and for PAGAWS, SS = 0.0096, 0.0043, and 4.95 for mean, s.d., and skew, respectively). On the basis of SS the PA5TR means were about 20% less accurate than those for PAGAWS. The PA5TR standard deviation and skewness matched the observed value best. However, the distributions were poorly reproduced (Table 5). The null hypothesis was rejected on six and four reaches for PAGAWS and PA5TR, respectively. A general trend, seen on Figures 10 and 11, is that simulated skew was less than observed for many of the rejected distributions. The value of D (Table 5) on seven of the ten rejections occurred at PA between 0.2 and 0.4. On these, original PA was less than 0.4. Cabin D, with the highest PA, was also rejected. This suggests that more inaccuracies occur as PA differs from 0.5.

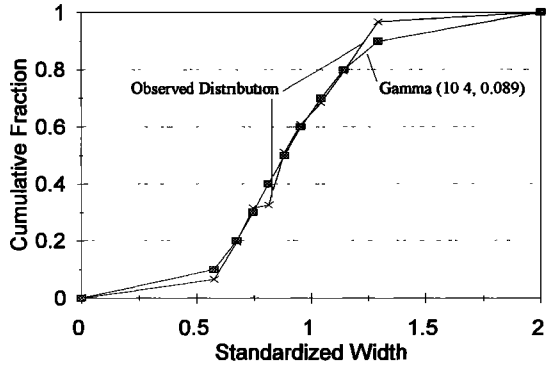

Figure 5. Comparison of the fit gamma distribution for water width with the observed for Cabin U with no pools.

Generally, the model reproduced standard deviation well indicating good reproduction of the variation about the mean. Both observed and modeled standard deviation tended to be higher for PA5TR than PAGAWS (compare Figures 8b and 9b). Considering that (1) may be expressed as

$$PA = \frac{1}{n\overline{WW}} \sum_{i=1}^{n} WW_i PF_i \tag{18}$$

then [*Dudewicz and Mishra*, 1988]:

$$\text{Var (PA)} = \sum_{i=1}^{n} \left(\frac{1}{n\overline{WW}}\right)^2 \text{Var (WW}_i\text{PF}_i\text{)}$$

$$+ 2 \sum_{i<j} \frac{1}{(n\overline{WW})^2} \text{Cov (WW}_i\text{PF}_i\text{, WW}_j\text{PF}_j\text{)} \tag{19}$$

Because WW generally exhibited significant autocorrelation at one lag (Table 1) and Markov chains adequately model PF transitions from transect-to-transect (Table 2), Cov (WW_iPF_i, WW_jPF_j) for $I = j - 1$ and the second half of the right-hand side of (19) is not equal to 0. Therefore sampling with adjacent transects has higher variance than lagging transects for which Cov (WW_iPF_i, WW_jPF_j) $\rightarrow$ 0.

Acceptable agreement on different streams resulted for different reasons. On Willow C (Figure 10) it resulted because discrepancies in categories balanced each other yielding equivalent means and densities on each side of the mean. The differences between simulated and observed PA means were due to smoothing as seen for Cabin D which had the poorest agreement (Figure 11). For both sampling schemes the observed fraction was 60% higher than simulated in the range 0.6–0.7, while the simulated fraction was 50 and 15% higher in the 0.7–0.8 and 0.8–0.9 ranges, respectively.

Table 4. Gamma Distribution Parameters (α, β) Estimated by the Method of Moments and χ^2 Goodness-of-Fit Comparison With Empirical Distributions for Standardized Stream Width

Reach	Pool Category	n	α	β	χ^2	P
Smith U	0	101	7.65	0.131	5.26	0.812
	1	32	11.1	0.078	5.50	0.789
	2	65	20.2	0.053	4.38	0.884
Smith D	0	64	17.3	0.060	5.69	0.771
	1	70	19.3	0.049	15.0	0.090
	2	29	16.1	0.064	12.7	0.175
Reese R	0	14	40.5	0.024	t.l.[a]	
	1	26	27.9	0.035	5.54	0.785
	2	23	30.6	0.034	6.13	0.727
Big Den D	0	86	8.39	0.112	11.3	0.252
	1	8	19.1	0.492	i.o.[b]	
	2	57	8.81	0.124	9.58	0.385
Big Den U	0	75	7.69	0.131	5.66	0.773
	1	28	6.74	0.121	4.14	0.902
	2	48	6.85	0.161	8.66	0.469
Big Meadow	0	64	6.29	0.159	11.3	0.255
	1	145	6.98	0.13	9.97	0.353
	2	42	7.92	0.155	21.3	0.011
Cabin D	0	16	5.61	0.15	i.o.[b]	
	1	67	9.59	0.10	11.0	0.278
	2	21	9.18	0.139	7.10	0.627
Cabin U	0	90	10.4	0.09	26.0	0.002
	1	73	10.7	0.10	8.51	0.484
	2	29	19.4	0.059	13.4	0.145
Mahogany	0	69	8.24	0.12	5.64	0.776
	1	52	9.29	0.10	6.75	0.663
	2	48	12.6	0.091	3.67	0.932
Summer Camp	0	67	11.4	0.00	8.37	0.497
	1	17	14.1	0.06	i.o.[b]	
	2	42	13.3	0.082	4.67	0.862
Washington	0	51	15.5	0.067	8.80	0.456
	1	36	17.0	0.05	10.1	0.342
	2	61	13.4	0.079	7.69	0.566
Willow	0	105	8.29	0.12	16.0	0.066
	1	50	12.2	0.07	13.6	0.137
	2	44	14.0	0.078	6.53	0.685

P, significance probability; n, number of transects. Pool categories are 0 (no pools), 1 (total pools), and 2 (partial pools). Test categories $K = 10$, and $df = 9$.

[a]The parameter α is too large, and the gamma function overflows on the computer.

[b]Insufficient observations: expected observations <2.

Skewness in a sample is high when just a few observations are much higher or lower than the mean. The observed skew of Big Den D (reach 4, Figures 8c and 9c) is much higher than simulated. This caused the high SS for skew. On Big Den D, several observed PA values (Figure 12) were more than 75% higher than the mean due to one cluster of small pools (between stations 105 and 120, Figure 2). That the simulation reproduced two spikes in the histogram illustrates the flexibility of the model. However, because of smoothing, there is much more density under the simulated curve near the spikes than under the observed spikes which causes the much lower skew. Models with continuous distributions would never perfectly match situations like Big Den U.

Stochastic Homogeneity and Scale

Throughout, we have assumed without testing that the study reaches were stochastically homogeneous. However, spikes observed in histograms of observed PA values and much higher skewness coefficients on some streams suggests that not all reaches are homogeneous. On the basis of other analyses we suggested that the maximum length for homogeneity is about 30 channel widths [*Myers*, 1996]. It is well known that width increases with flow [*Leopold and Maddock*, 1953] or drainage area [*Klein*, 1981], but our reaches are short, and there is no substantial change in flow or drainage area. Inhomogeneous conditions should be indicated by trends or shifts in mean values over these short reaches.

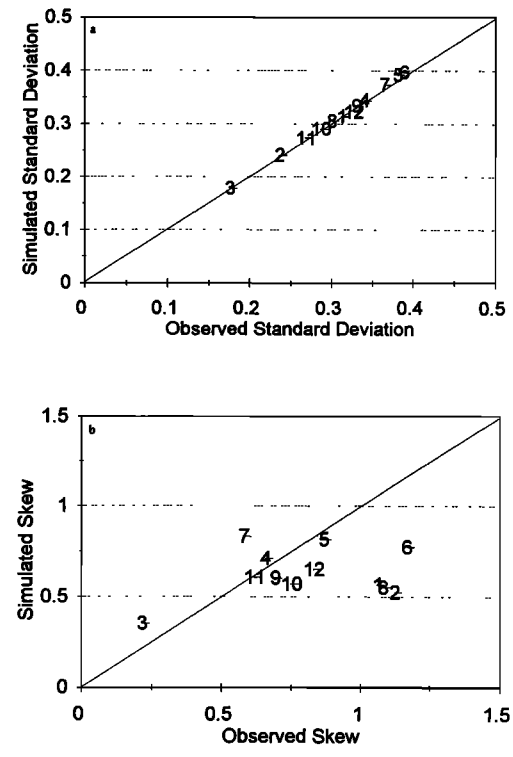

Figure 6. Comparison of observed and simulated water width (a) standard deviation and (b) skewness. The numbers represent reach numbers.

Because width measurements fit a gamma distribution, we used a simple linear rank regression model of WW and CW with station along reaches to test for trend [*Conover and Iman*, 1981]. We tested for shifts by dividing the reaches into segments of 30 transects and testing for differences in the distribution of WW, CW, PF, and WW_tPF_t (a surrogate for PA at

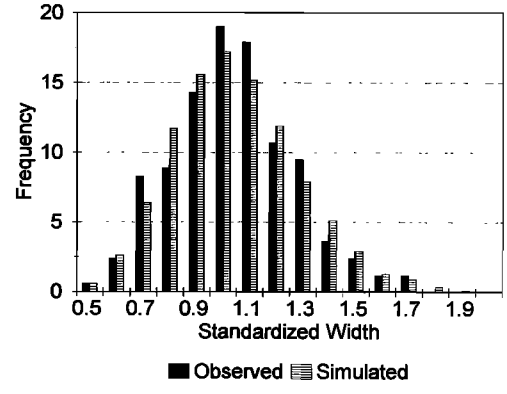

Figure 7. Comparison of observed and simulated water width for Smith D.

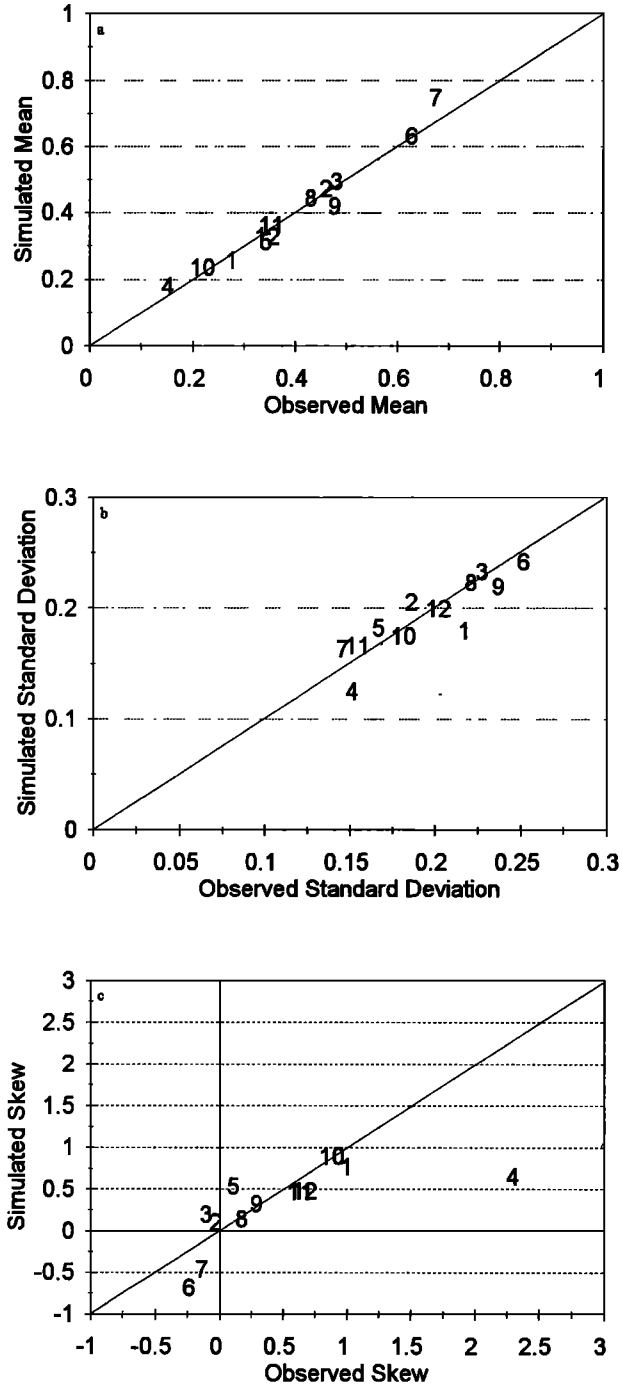

Figure 8. Comparison of observed and simulated moments for PA5TR. The numbers are reach number labels. (a) Mean, (b) standard deviation, and (c) skewness.

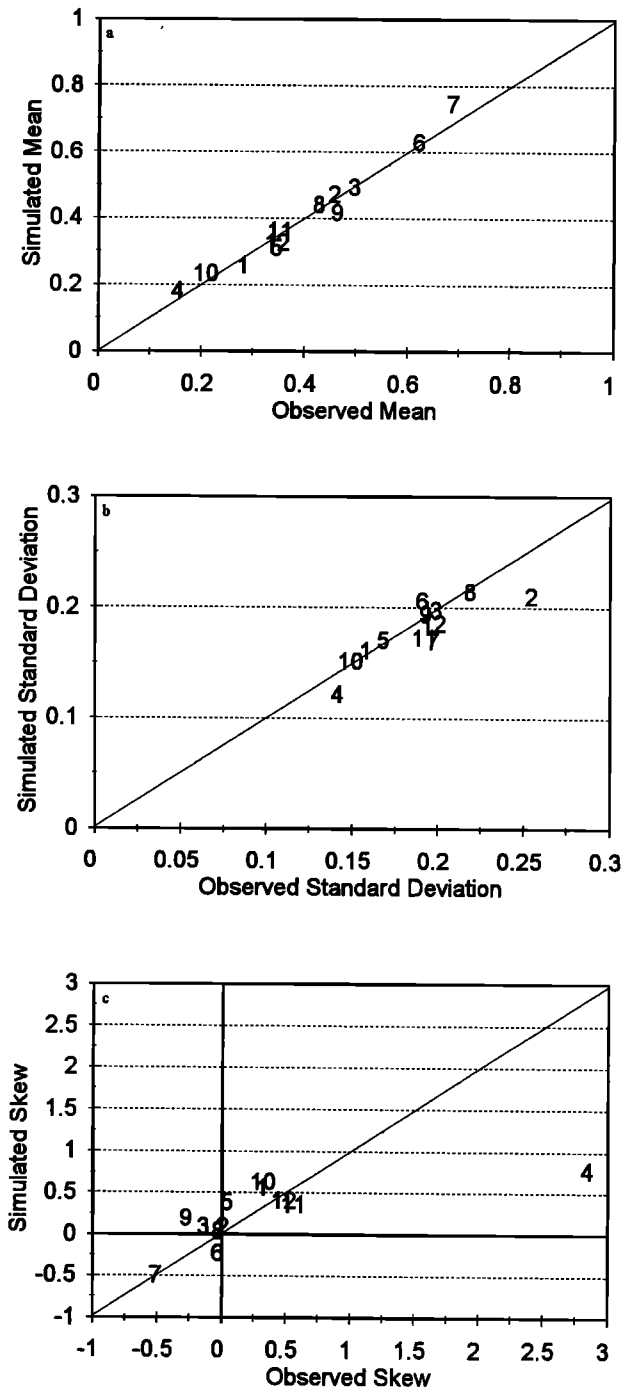

Figure 9. Comparison of observed and simulated moments for PAGAWS. The numbers are reach number labels. Parts of figure are as in Figure 8.

the one-transect scale; it is standardized pool width) with Kruskal-Wallis one-way nonparametric ANOVA [*Sokal and Rohlf*, 1981] and with Mann-Whitney *U* tests for Reese R which had only two 30-transect segments. Significant coefficients in the regression indicate trends along the reach, and different distributions indicate shifts.

The results (Table 6) suggest that inhomogeneity of long reaches for either width may be a problem. Widths trended on about 38% of the reaches, although the slope of CW was significant more often than the slope of WW. Widths shifted on about 54% of the reaches again with slightly more frequency for channel widths. Randomness such as windthrow and soil or vegetation cover type change apparently affects the channel width more than the water width. This corresponds with higher CV for channel widths. Shifts among subreaches lead to significant regression coefficients if the shifts do not cancel each other.

The distributions of both PF and pool width shifted significantly only on Big Meadow (Table 6). This suggests that PA is stationary throughout the range of streams studied here. That

Table 5. Comparison of Simulated and Observed PA Values

Reach	PA5TR		PAGAWS	
	n	*D*	*n*	*D*
Smith U	195	0.072	180	0.122[a]
Smith D	164	0.067	149	0.076
Reese R	59	0.034	44	0.067
Big Den D	147	0.223[a]	132	0.227[a]
Big Den U	147	0.103[a]	132	0.122[a]
Big Meadow	247	0.035	232	0.035
Cabin D	100	0.226[a]	85	0.148[a]
Cabin U	190	0.051	175	0.048
Mahogany	165	0.114[a]	150	0.141[a]
Summer Camp	122	0.097	106	0.059
Washington	145	0.039	130	0.114[a]
Willow	195	0.070	180	0.058

PA5TR, pool area based on five transects spaced one transect apart; PAGAWS, pool area based on five transects spaced four transects apart; D, Kolmogorov-Smirnoff test statistic; *n*, number of PA representations in the observed reach.

[a] $D > D_1 = \frac{1.22}{\sqrt{n}}$ [*Haan*, 1977].

pool width shifted on only one reach even when the WW portion of the variable shifted on 50% of reaches indicates that pool location and size control the homogeneity of PA. Control of PA by PF should be expected because PF variability ($0 \leq PF \leq 1$) exceeds WW variability (CV < 50%).

On Big Meadow, although WW and PF trended in opposite directions (Figure 13), pool width paralleled PF. Shifts in both water and channel width are obvious toward the upstream end

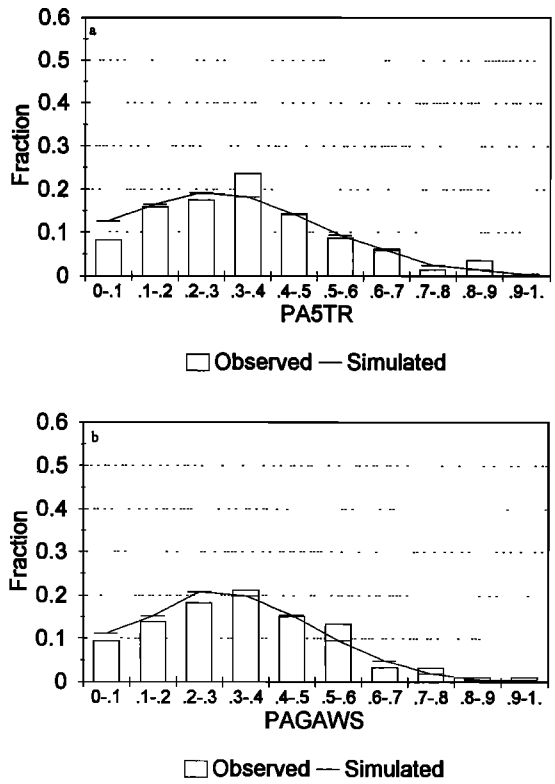

Figure 10. Comparison of observed and simulated PA values for Willow C for each sampling scheme. (a) PA5TR and (b) PAGAWS.

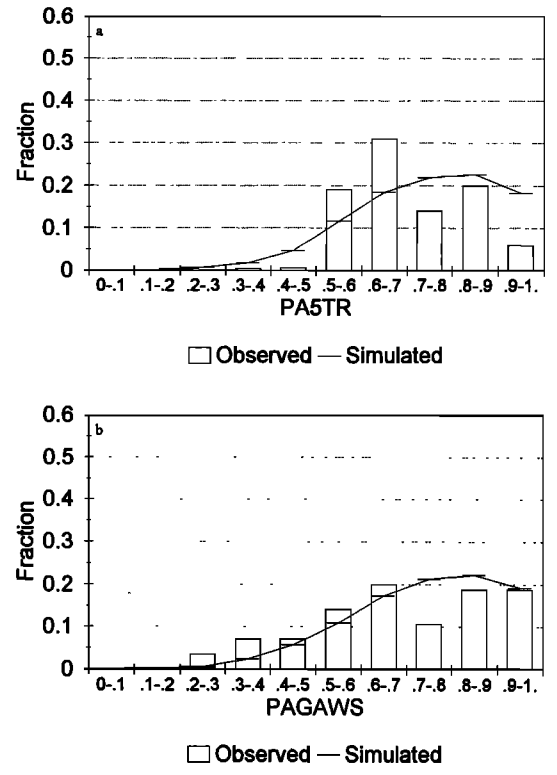

Figure 11. Comparison of observed and simulated PA values for Cabin D for each sampling scheme. Parts of figure are as in Figure 10.

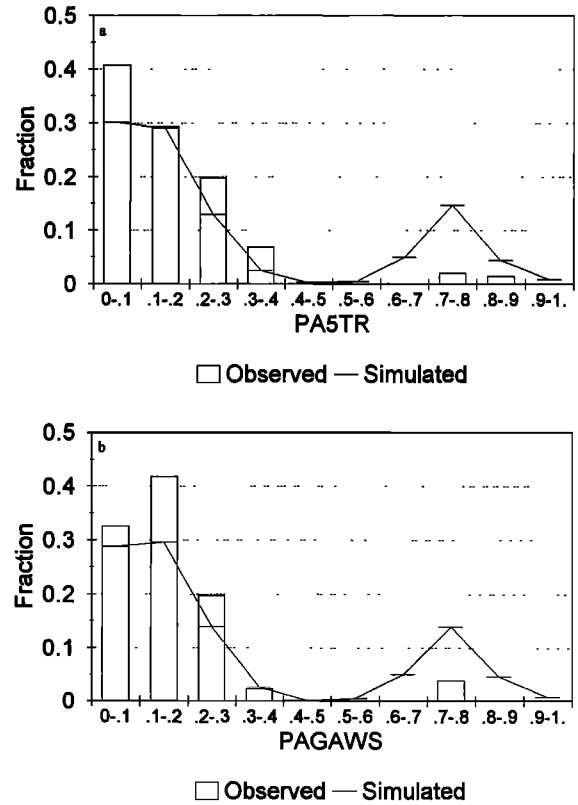

Figure 12. Comparison of observed and simulated PA values for Big Den D for each sampling scheme. Parts of figure are as in Figure 10.

Table 6. Slope of Simple Regression Model for Water Width and Channel Width, One-Way ANOVA for WW and CW, and Kruskal Wallis One-Way ANOVA for Pool Fraction and Pool Width

	Rank Regression		Kruskal-Wallis Test Statistic			
Reach	WW Coefficient	CW Coefficient	WW	CW	PF	Pool Width
Smith U	−3.06	−4.26[a]	21.30[b]	34.20[b]	10.10	8.99
Smith D	−9.39[b]	2.64	14.40[c]	11.80[c]	3.08	5.30
Reese R	−3.67[c]	−1.14	2.74[b,d]	0.49[d]	0.55[e]	0.95[e]
Big Den D	5.14	−4.51	4.10	14.50[b]	3.93	3.56
Big Den U	2.15	0.38	9.29[a]	6.73	1.81	2.49
Big Meadow	8.92[c]	15.30[b]	39.70[b]	55.20[b]	32.90[b]	26.40[b]
Cabin D	2.61	−7.00[b]	6.58[a]	4.13[c]	1.72	7.79[c]
Cabin U	2.53	−4.65	5.79	13.70[b]	0.90	0.88
Mahogany	0.09	5.18[c]	8.41	24.10[b]	4.95	5.04
Summer Camp	−2.07	−0.85	2.48	4.70	2.41	2.15
Washington	−5.78[a]	−5.58[a]	12.60[c]	10.60[c]	5.20	4.59
Willow	2.59	6.33[c]	12.20[a]	14.0[c]	9.23	7.91

Slope is times 10^4. WW, water width; CW, channel width; PF, pool fraction; WW_tPF_t, pool width; ANOVA, analysis of variance.
[a] $P \leq 0.10$.
[b] $P \leq 0.01$.
[c] $P \leq 0.05$.
[d] T test statistic because there are only two groups.
[e] Mann-Whitney U statistic because there are only two groups.

with much higher variability for channel width (Figure 13a). That there are fewer pools at the upper end is also apparent (Figure 13b). The pool width more closely parallels PF than WW. Big Meadow is therefore a reach specific example of how homogeneity of pool width depends more on pools than width.

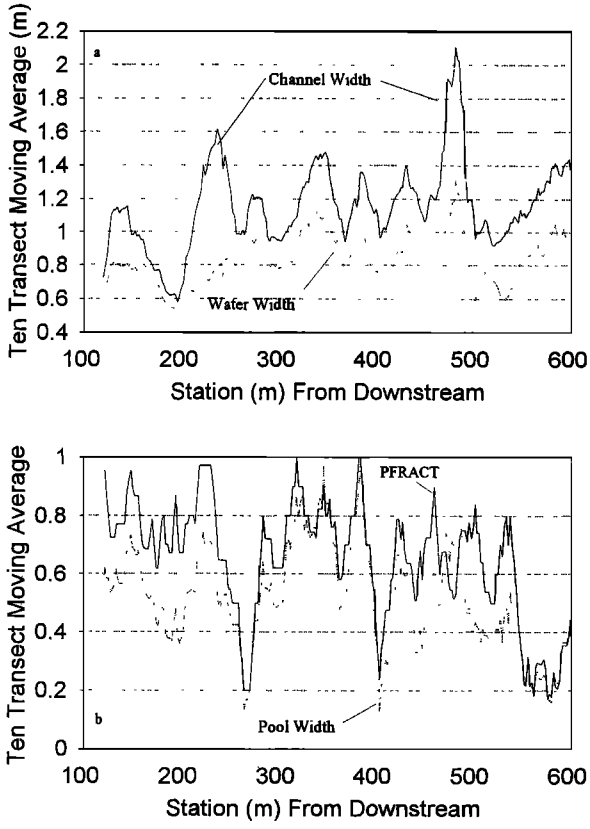

Figure 13. Series of (a) channel and water width and (b) pool width and fraction for Big Meadow.

Conclusion

We presented an eight-parameter Markov chain based stochastic model of transect-to-transect properties that accurately reproduced width and pool characteristics of 12 variable rangeland streams in Nevada. The WW and PF parameters have physical significance allowing a user to simulate a variety of streams. The model simulated a wide variety of small, stochastically homogeneous streams by reproducing the first and second moments of both water width and PA. Higher-order moments and exact distributions in real streams are not perfectly reproduced. However, smoothing of partially discrete data modeled with continuous distributions and inhomogeneities along the reach caused most of the discrepancies.

This model could be used to test sampling strategies. A user could determine the best transect spacing and optimal number of transects based on geomorphic variability as represented by stochastic parameters. The documented success of the model with a wide variety of small streams indicates that the model performs satisfactorily.

Acknowledgments. This research was funded by a Federal Aid in Sport Fish Restoration grant from the Nevada Division of Wildlife and funds from the Nevada Agricultural Experiment Stations Project 52DM. We thank E. A. Keller and an anonymous reviewer as well as G. Fred Gifford, Dale F. Ritter, Elizabeth Jacobsen, and John Warwick for review and service on the senior author's Ph.D. committee.

References

Acreman, M. C., A simple stochastic model of hourly rainfall for Farnborough, England, *Hydrol. Sci. J.*, *35*, 119–148, 1990.

Alexander, C. O., and H. Rendell, Data generation processes for spatial series: The example of ephemeral channel form, *Geogr. Anal.*, *27*, 78–93, 1995.

Bobée, B., and F. Ashkar, *The Gamma Family and Derived Distributions Applied in Hydrology*, 203 pp., Water Resour. Publ., Fort Collins, Colo., 1991.

Conover, W. J., and R. L. Iman, Rank transformations as a bridge

between parametric and nonparametric statistics, *Am. Stat.*, *35*, 124–129, 1981.

Dudewicz, E. J., and S. N. Mishra, *Modern Mathematical Statistics*, 838 pp., John Wiley, New York, 1988.

Gabriel, K. R., and J. Neumann, A Markov chain model for rainfall occurrence, *Q. J. R. Meteorol. Soc.*, *83*, 375–380, 1962.

Grant, G. E., F. J. Swanson, and M. G. Wolman, Pattern and origin of stepped-bed morphology in high-gradient streams, Western Cascades, Oregon, *Geol. Soc. Am. Bull.*, *102*, 340–352, 1990.

Haan, C. T., *Statistical Methods in Hydrology*, 378 pp., Iowa State Univ. Press, Amers, 1977.

Haan, C. T., D. M. Allen, and J. O. Street, A Markov model of daily rainfall, *Water Resour. Res.*, *12*, 443–449, 1976.

Haktanir, T., and N. Sezen, Suitability of two-parameter gamma and three-parameter beta distributions as synthetic unit hydrographs in Anatolia, *Hydrol. Sci. J.*, *35*, 167–184, 1990.

Hankin, D. G., and G. H. Reeves, Estimating total fish abundance and total habitat area in small streams based on visual estimation methods, *Can. J. Fish. Aquat. Sci.*, *45*, 834–844, 1988.

Harvey, A. M., Some aspects of the relations between channel characteristics and riffle spacing in meandering streams, *Am. J. Sci.*, *275*, 470–478, 1975.

Keller, E. A., Areal sorting of bed-load material: The hypothesis of velocity reversal, *Geol. Soc. Am. Bull.*, *83*, 1531–1536, 1971.

Keller, E. A., and F. J. Swanson, Effects of large organic material on channel form and fluvial processes, *Earth Surf. Processes*, *4*, 361–380, 1979.

Kirchner, J. W., Statistical inevitability of Horton's laws and the apparent randomness of stream channel networks, *Geology*, *21*, 591–594, 1993.

Klein, M., Drainage area and the variation of channel geometry downstream, *Earth Surf. Processes Landforms*, *6*, 589–593, 1981.

Law, A. M., and W. D. Kelton, *Simulation Modeling and Analysis*, 759 pp., McGraw-Hill, New York, 1991.

Leopold, L. B., *A View of the River*, Harvard Univ. Press, Cambridge, Mass., 1994.

Leopold, L. B., and W. B. Langbein, The concept of entropy in landscape evolution, *U.S. Geol. Surv. Prof. Pap.*, *500-A*, 1962.

Leopold, L. B., and T. Maddock, The hydraulic geometry of stream channels and some physiographic implications, *U.S. Geol. Surv. Prof. Pap.*, *252*, 56 pp., 1953.

Mielke, P. W., Jr., and E. S. Johnson, Some generalized beta distributions of the second kind having desirable application features in hydrology and meteorology, *Water Resour. Res.*, *10*, 223–226, 1974.

Mosley, M. P., and A. I. McKerchar, Streamflow, in *Handbook of Hydrology*, edited by D. R. Maidment, chap. 8, pp. 8.1–8.39, McGraw-Hill, New York, 1993.

Murgatroyd, A. L., and J. L. Ternan, The impact of afforestation on stream bank erosion and channel form, *Earth Surf. Processes Landforms*, *8*, 357–369, 1983.

Myers, T. J., Stochastic structure of rangeland streams, Ph.D. dissertation, Univ. of Nev., Reno, 1996.

Myers, T. J., and S. Swanson, Aquatic habitat condition index, stream type, and livestock bank damage in northern Nevada, *Water Resour. Bull.*, *28*, 743–754, 1991.

Myers, T., and S. Swanson, Grazing effects on pool forming features in central Nevada, in *Effects of Human-Induced Changes on Hydrologic Systems*, edited by R. A. Marston and V. R. Hasfurther, pp. 235–244, Am. Water Resour. Assoc., Jackson Hole, Wyo., 1994.

Myers, T. J., and S. Swanson, Long-term aquatic habitat restoration: Mahogany Creek, Nevada, as a case study, *Water Resour. Bull.*, *32*, 241–252, 1996.

Myers, T. J., and S. Swanson, Stream morphologic impact of and recovery from catastrophic flooding in north-central Nevada, *Phys. Geogr.*, *17*, 431–445, 1996.

Phillips, P. J., and J. M. Harlin, Spatial dependence of hydraulic geometry exponents in a subalpine stream, *J. Hydrol.*, *71*, 277–283, 1984.

Pickup, G., and W. A. Rieger, A conceptual model of the relationship between channel characteristics and discharge, *Earth Surf. Processes*, *4*, 37–42, 1979.

Press, W. H., S. A. Teukolsky, W. T. Vetterling, and B. P. Flannery, *Numerical Recipes in Fortran: The Art of Scientific Computing*, 2nd ed., 963 pp., Cambridge Univ. Press, New York, 1992.

Price, W. E., Simulation of alluvial fan deposition by a random walk model, *Water Resour. Res.*, *10*, 263–274, 1974.

Rendell, H., and D. Alexander, Note on some spatial and temporal variations in ephemeral channel form, *Geol. Soc. Am. Bull.*, *90*, 761–772, 1979.

Richards, K. S., Channel width and the riffle-pool sequence, *Geol. Soc. Am. Bull.*, *87*, 883–890, 1976.

Richards, K. S., *Rivers: Form and Process in Alluvial Channels*, 361 pp., Methuen, New York, 1982.

Robison, E. G., and R. L. Beschta, Coarse woody debris and channel morphology interactions for undisturbed streams in southeast Alaska, U.S.A., *Earth Surf. Processes Landforms*, *15*, 149–156, 1990.

Robison, E. G., and J. B. Kaufman, Comparison of two techniques for determining pools, in *Effects of Human-Induced Changes on Hydrologic Systems*, edited by R. A. Marsten and V. R. Hasfurther, pp. 689–698, Am. Water Resour. Assoc., Jackson Hole, Wyo., 1994.

Rosgen, D. L., A classification of natural rivers, *Catena*, *22*, 169–199, 1994.

Ross, S. M., *Stochastic Processes*, 309 pp., John Wiley, New York, 1982.

Shreve, R. L., Variation of mainstream length with basin area in river networks, *Water Resour. Res.*, *10*, 1167–1177, 1974.

Singh, V. P., *Hydrologic Systems: Rainfall-Runoff Modeling*, vol. 1, 480 pp., Prentice-Hall, Englewood Cliffs, N. J., 1988.

Sokal, R. R., and F. J. Rohlf, *Biometry: The Principles and Practice of Statistics in Biological Research*, 859 pp., W. H. Freeman, New York, 1981.

Stewart, J. H., and J. E. Carlson, *Geologic Map of Nevada*, U.S. Geol. Surv., Carson City, Nev., 1978.

Thompson, S. A., A Markov and runs analysis of drought in the central United States, *Phys. Geogr.*, *11*, 191–205, 1990.

U.S. Forest Service (USFS), Fisheries habitat survey handbook, *USFS Intermt. Reg. Rep. (94)-FSH 2609-23*, Ogden, Utah, 1985.

Williams, G. P., Bank-full discharge of rivers, *Water Resour. Res.*, *14*, 1141–1154, 1978.

Yakowitz, S. J., Markov flow models and the flood warning problem, *Water Resour. Res.*, *21*, 81–88, 1985.

Yapo, P., S. Sorooshian, and V. Gupta, A Markov chain flow model for flood forecasting, *Water Resour. Res.*, *29*, 2427–2436, 1993.

Yevjevich, V., and N. B. Harmancioğlu, Periodic-stochastic modeling of separation of precipitation into rainfall and snowfall, *Water Resour. Res.*, *26*, 2613–2623, 1990.

T. J. Myers and S. Swanson, Department of Environmental and Resource Sciences, University of Nevada, Reno, 1000 Valley Road, Reno, NV 89512. (e-mail: tjmyers@unr.edu; sswanson@fs.scs.unr.edu)

(Received April 15, 1996; revised December 17, 1996; accepted December 26, 1996.)